A NOVEL SPATIAL POOLING TECHNIQUE FOR IMAGE QUALITY ASSESSMENT BASED ON LUMINANCE-CONTRAST DEPENDENCE

V. Bruni[1,2], *D. Vitulano*[2]

[1]Dept of SBAI, Univ. of Rome La Sapienza
[2] I.A.C. - CNR
Rome, Italy

Z. Wang

Dept. of ECE,
Univ. of Waterloo
Waterloo, Canada

ABSTRACT

The paper presents a spatial pooling technique for image quality assessment (IQA) that is based on the idea that the adaptive mechanisms of luminance and contrast in the early vision operate independently. The work is motivated by recent vision science studies on this topic that have not been investigated yet in the field of IQA. The Structural SIMilarity index (SSIM) has been selected as the base IQA measure due to its explicit utilization of the local luminance mean and contrast of both original and degraded images. Experimental results show that a spatial pooling algorithm that only depends on the degraded image results in significantly improved image quality prediction.

***Index Terms*—** Image quality assessment, spatial pooling, visual contrast, fixation points, SSIM

1. INTRODUCTION

In the last years a lot of work has been done for defining quality measures that correlate with Human Visual System (see [14, 12] for a brief review). This is not a trivial problem due to the partial knowledge and lack of theoretical models of brain activities in the presence of visual stimuli. Even though the subjective aspect in human vision is difficult to predict, it has been widely recognized that not all image pixels have the same importance in the visual perception process. With regard to image quality assessment (IQA), this concept has been translated into the definition of proper spatial pooling techniques, which define the global image quality score as a weighted mean of local image quality and tune the weights according to the visual importance of each image region. Although the effectiveness of spatial pooling strategies has been demostrated in several recent papers, some of them are not built up on human visual characteristics while some others require a high computational load.

This paper presents a novel study oriented to the definition of a pooling method which measures the naturalness of local image patches. This study is inspired by the strong results reported in [5, 7] and related works about the independence of the adaptive mechanisms of luminance and contrast of natural images and the low spatial correlation of these measures near fixation points. As a result, by looking at image defects as artificial (and thus unnatural) image components, the main idea of this work is to assign a higher weight to image regions that are highly unnatural and are surprisals to the human visual system. To this aim, the well known and widely used IQA metric, namely the Strucutral SIMIilarity index (SSIM [16]), has been selected as the base IQA measure. The main motivations are: *i)* SSIM is directly dependent on the two main measures adopted by human eye in the observation process, i.e. local luminance mean and contrast [7, 5]; *ii)* SSIM creates local quality maps that allow for straightforward spatial pooling. In addition, SSIM has got other interesting properties that further support its choice in this preliminary study: *i)* it is computationally efficient; *ii)* its mathematical properties make it easily embeddable in several image and video processing applications; *iii)* it gives considerable importance to the modification of image structures to which HVS is sensitive (i.e. object contours). Experimental results are promising in terms of increased correlation between SSIM and mean opinion score (MOS) and reduced computational effort for the computation of the weights.

2. LUMINANCE-CONTRAST INDEPENDENCE AS PERCEPTUAL POOLING STRATEGY

There has been a rich literature recently regarding perception-based pooling strategies for SSIM. For example, the work in [10] uses gaze to assign more importance to points that are fixated with high probability; the same work, as well as the one in [1], also relies on the theory that human eye is highly influenced by the worst regions of the image; on the contrary in [18], based on the fact that object contours attract human attention, the distribution of edges in the original and degraded image is used for pooling; edge map and phase coherence are the main properties of the Feature-SIM presented in [19], that has the same mathematical form of SSIM but it involves different variables that are more consistent with HVS; finally, in [11] pooling is performed in the wavelet domain according to the contrast amplitude of the original image and using a corrective term that depends on the edge map. In order to characterize informative image points, we mainly focus on the relationship between image local luminance and contrast in the early vision and their typical behavior in correspondence to fixation points. The motivations for this choice are elaborated in the next section.

2.1. Motivations

As pointed out in [5, 7], during the observation of a scene the eye essentially measures local *luminance mean* and *contrast*. Specifically, light adaptation (luminance gain) and contrast gain are the two rapid mechanisms that control the gain of neural responses in the early vision. Light adaptation largely occurs in the retina and normalizes the local luminance with respect to the prevalent one; on the contrary, contrast gain starts in the retina and reduces neural responses where contrast is high while increases them where contrast is low. From a more formal point of view, luminance and contrast are related to local and global image statistics that can be restricted, in most cases, to those of the first and second order, i.e. mean μ and variance σ^2 of the image luminance. In particular, the visual contrast is well represented by the ratio of these statistics, i.e. $C = \frac{\sigma}{\mu}$. The most interesting result of the works in [5, 7] is the empirical observation of a nearly statistical independence of local luminance and contrast in natural images and a highly negative correlation of those measures in artificial images with matched spectral characteristics. In addition, luminance and contrast can significantly vary in the whole image so that their local values are predictable only for very close observation points. To support these statements, independence of luminance and contrast gain control mechanisms has been thoroughly studied in several experiments [5, 7]. Interestingly, by fixing the amplitude and changing randomly the phase of images, the authors observed that luminance and contrast are far from independent; on the contrary, by preserving image structures (the phase) of natural images and changing the amplitude, luminance and contrast result largely statistical independent. To this aim the authors computed the empirical joint distributions between local luminance mean and contrast in natural images, that include both rural and urban areas, and showed their near separability. However, to quantify the amount of independence between the two involved quantities, they measured the Pearson correlation coefficient ρ between local luminance and contrast. Even though Pearson correlation coefficient is commonly used for its simplicity and low computational cost, uncorrelated random variables are not necessarily independent. Mutual information is a more proper measure for the independence of two random variables (luminance mean μ and contrast C in our case) since it quantifies how much information the two variables share. Specifically, it is defined as $I(C, \mu) = H(C) - H(\mu|C) = H(C) + H(\mu) - H(C, \mu)$ and equals zero if and only if the two random variables are

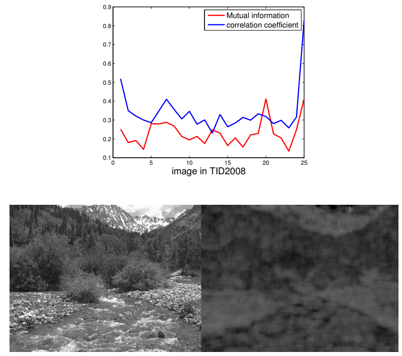

Fig. 1. TID2008. **Top)** Average mutual information (*topmost curve*) and Pearson correlation coefficient (*bottommost curve*) between local luminance mean and contrast for each original image in the database. **Bottom)** Image no. 13 (*left*), that is a typical natural image, and the mutual information map of its local luminance mean and contrast (*right*).

independent. In addition, if C and μ have a joint normal distribution, that is the one that seems to approximate well the relationship between local luminance mean and contrast (see Figures 2 and 5 respectively in [7, 5]), I and ρ obey the following rule: $I(C, \mu) = -\frac{1}{2} log(1 - \rho^2(C, \mu))$. Based on this last observation, to further confirm the results in [5, 7], we computed the local mutual information between luminance and contrast of the images in TID database. As it can be observed in Fig. 1.top, the average normalized mutual information ($H(C) + H(\mu)$ has been used for normalization) is 0.2309 and for most of the images it is less than 0.3. It is worth observing that many images in the database have several natural components (sky, foliage, backlit, ground), as the image in Fig. 1.bottom, while one of the highest values of the average mutual information is assumed by the last image in the database, which is an artificial image. For the same image the average value of the Pearson correlation coefficient assumes a high value, as shown in Fig. 1.top. Fig. 1.top also shows a quite similar behaviour of mutual information and Pearson correlation coefficient in the database. Since the evaluation of the mutual information is costly, in the remaining part of the paper we will focus on the correlation coefficient between local luminance and contrast.

2.2. Image unnaturalness for pooling

As discussed in the previous section, the correlation between luminance mean and contrast can be a discriminative feature for points that attract human attention during the observation process of a natural image. In fact, on the one hand it allows us to characterize those regions with which human eye is very familiar (ρ is close to zero), and therefore more sensitive to their quality; on the other hand, it allows us to detect unnat-

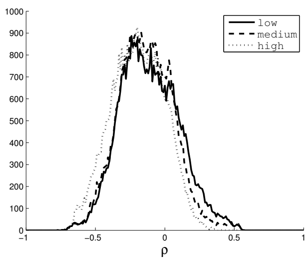

Fig. 2. TID database: histograms of ρ for the image no. 13 affected by jpeg transmission distortion. Three levels of distortions have been considered. ρ moves toward negative values as the amount of distortion increases.

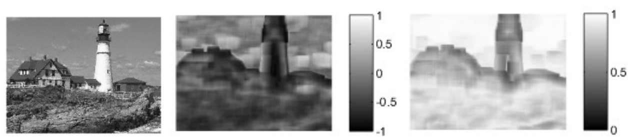

Fig. 3. Image 20 of TID database (*left*), its ρ image (*middle*), its ρ_{cos} image (*right*).

ural image elements that can influence the perception of the quality of the whole image, since anomaluos image components (almost large negative correlation). In agreement with the studies in [10], in which it has been assessed that humans are attracted by the most unnatural parts of the image, a perception based spatial pooling method has to assign a higher weight to those points in the image that have higher negative correlation between luminance and contrast, since they are more likely to be unnnatural image components. As a consequence, local SSIM values can be weighted by the quantity $1-\rho$ as follows

$$SSIM_\rho = \frac{\sum_{x=1}^{n}\sum_{y=1}^{m} SSIM(x,y)(1-\rho(x,y))}{\sum_{x=1}^{n}\sum_{y=1}^{m}(1-\rho(x,y))}, \quad (1)$$

where (x, y) indicates pixel locations, $n \times m$ is the image dimension and $SSIM(x, y)$ is the SSIM value computed in a block centered at (x, y). Note that ρ is taken with its sign. As a result, the more unnatural the image, the higher the weight for the corresponding SSIM value. It is obvious that, for a pooling method which is consistent with HVS, the correlation coefficient ρ in eq. (1) must refer to local luminance and contrast of the degraded image since degradation introduces artificial structures that do not belong to the original image. Fig. 2 shows the histograms of the correlation coefficient computed in image no. 13 of TID database corrupted by JPEG transmission errors. As it can be observed, the higher the amount of distortion the more the correlation coefficients between luminance mean and contrast of the degraded image move toward negative values. This is also consistent with the fact that the locations of fixation points in the observation process change according to both the image content [2] and image distortion type [15]. In fact, as shown in the experiments presented in [15] and performed on LIVE database, fixations in the degraded image change especially for compression distortions as they move to edges and/or blocking artifacts. On the contrary, for distortions like white noise or Gaussian blurring, fixations do not significantly change, even when they occur in homogeneous regions, where the degradation is easily detectable.

2.3. Refinements in weight estimation

Pearson correlation coefficient captures linear dependence between two variables but ignores any other kind of dependence. In order to establish a better statistical correlation between luminance mean and contrast, a more sophisticated statistical model should be used and an a priori information on the conditional probability between the two variables should be introduced. Unfortunately, such information is neither available nor well assessed empirically yet, even though in [3] some constraints on the density functions of luminance and contrast have been assessed. Here we opt to a deterministic approach to evaluate the independence between the two involved variables. We select a patch and we extract a sample of luminance mean and contrast. Each sample is seen as a vector in the n-dimensional space and then we look at the angle between the two vectors through the cosine correlation coefficient

$$\rho_{cos}(x,y) = \frac{\sum_{(x,y)\in\Omega}\mu(x,y)C(x,y)}{\sqrt{\sum_{(x,y)\in\Omega}\mu^2(x,y)}\sqrt{\sum_{(x,y)\in\Omega}C^2(x,y)}}$$

where Ω is the considered patch. If luminance and contrast are independent, their corresponding vectors must be orthogonal and the cosine of the angle tends to zero; otherwise the cosine of the angle departs from zero. In this way we are implicitly considering the a priori information that human eye is inclined to take two different kinds of information (luminance and contrast) by means of two separate channels. This is consistent with the mechanisms of luminance and contrast gain control in early vision [5, 7]: the first one mainly involves the retina while the second one only begins in the retina but then it involves other stages in the visual pathway.

It is worth noting that the relationship between ρ and ρ_{cos} is not strictly linear but it depends on local image information. It is easy to derive that

$$\rho_{cos} = \frac{\|\mu\|_1\,\|C\|_1}{\|\mu\|_2\,\|C\|_2} + \rho\sqrt{\left(1-\frac{\|\mu\|_1^2}{\|\mu\|_2^2}\right)\left(1-\frac{\|C\|_1^2}{\|C\|_2^2}\right)},$$

where the dependence on the point location (x, y) has been omitted. Points having ρ close to zero (i.e. the ones more similar to natural image components) not necessarily have $\rho_{cos} = 0$; in this case $\rho_{cos} = \frac{\|\mu\|_1\|C\|_1}{\|\mu\|_2\|C\|_2}$ and it depends on the length of luminance and contrast vectors. For the same reasons, low values of ρ_{cos} with high probability are those

correlation	*DB*	$SSIM$	$SSIM_\rho$	$SSIM_{cos}$	VIF	FSIM	VSNR	$SSIM_\rho$ (from original)	$SSIM_{cos}$ (from original)
PCC	TID	0.773	0.795	*0.835*	0.808	**0.874**	0.682	0.746	0.772
	LIVE	0.945	0.948	*0.954*	0.960	**0.961**	0.923	0.946	0.949
	CSIQ	0.861	*0.890*	0.870	**0.928**	0.912	0.800	0.888	0.865
SCC	TID	0.775	0.795	*0.838*	0.749	**0.881**	0.705	0.780	0.805
	LIVE	0.948	0.952	*0.958*	0.964	**0.965**	0.927	0.949	0.953
	CSIQ	0.876	*0.904*	0.879	0.919	**0.924**	0.811	0.901	0.875
KCC	TID	0.577	0.595	*0.644*	0.586	**0.695**	0.534	0.582	0.609
	LIVE	0.796	0.805	*0.817*	0.827	**0.836**	0.762	0.799	0.807
	CSIQ	0.691	*0.724*	0.696	0.754	**0.757**	0.625	0.720	0.697

Table 1. Pearson (PCC), Spearman (SCC) and Kendall (KCC) correlation coefficients for SSIM, $SSIM_\rho$ and $SSIM_{cos}$, in TID, LIVE and CSIQ databases (best results are in italic). Pooling weights have been computed on the degraded images (*4th and 5th cols)* and on the original images (*last two columns)*. Cols 7,8 and 9 provide the results for three representative IQA metrics: VIF [13], VSNR [20] and FSIM [19] (best results are in bold).

points having negative correlation, since it means that a given quantity is subtracted from the term $\frac{\|\mu\|_1 \, \|C\|_1}{\|\mu\|_2 \|C\|_2}$. Hence, even though the cosine does not distinguish between points having positive or negative angles, the value of ρ_{cos} is able to differentiate, in principle, points having positive and negative correlations. As a result, local SSIM values can be weighted as follows

$$SSIM_{cos} = \frac{\sum_{x=1}^{n} \sum_{y=1}^{m} SSIM(x,y)(1-\rho_{cos}(x,y))}{\sum_{x=1}^{n} \sum_{y=1}^{m} (1-\rho_{cos}(x,y))} \tag{2}$$

An example is shown in Fig. 3. The cosine correlation ρ_{cos} between luminance and contrast is a more consistent with the perception of masked noise: noise is less evident at the bottom of the image than near the contours of the houses or the lighthouse; the values of ρ_{cos} vary accordingly whereas the values of ρ seem less dependent on this feature.

3. EXPERIMENTAL RESULTS

The proposed method has been tested on several images corrupted by different kinds of distortions taken from the three well known and publicly available databases CSIQ [6], LIVE [9] and TID2008 [8]. *Gaussian noise, blur, contrast alteration, pink noise, JPEG, JPEG2000* are the distortion types considered in CSIQ, while *Fastfading, Gaussian blur, JPEG, Gaussian noise* and *JPEG2000* are those in LIVE. A wider class of distortions has been considered in TID2008. The correlation with MOS on the three databases has been measured in terms of prediction accuracy through the Pearson correlation coefficient after non linear regression using the five parameters logistic function

$$Q_p = \alpha_1 \left(\frac{1}{2} - \frac{1}{1+e^{\alpha_2 (Q-\alpha_3)}} \right) + \alpha_4 Q + \alpha_5,$$

where $\{\alpha_1, \alpha_2, \ldots, \alpha_5\}$ are the regression parameters while Q and Q_r respectively are the original IQA metric and the one after regression; and also in terms of prediction monotonicity using both Spearman and Kendall correlation coefficients.

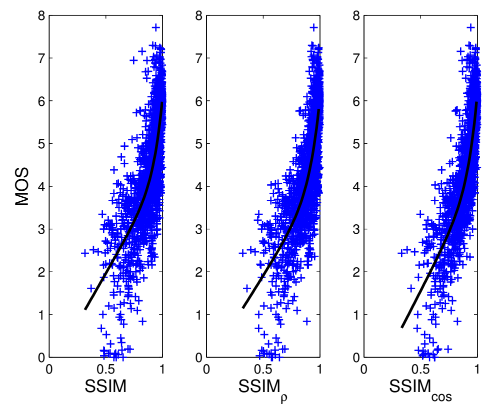

Fig. 4. TID database: Scatter plot of MOS versus SSIM and its two pooled versions. The black line is the fitted logistic function.

A block-shaped patch of dimension 32×32 has been considered for the computation of the local correlation between luminance and contrast, whose vectors have been defined by sampling the patch 1 out of 4 in both horizontal and vertical direction, i.e. each vector has 64 components. In each location (x, y) the luminance mean and contrast have been computed on a 4×4 block. It is worth mentioning that the results for $SSIM_{cos}$ do not significantly change if a different dimension of the patch is used. In addition a patch of 32×32 dimension corresponds to a visual angle of 0.54 degree and it is consistent with the default settings of SSIM computation. Table 1 shows the results for the two proposed spatial pooling methods in eqs. (1) and (2) and compares them with the conventional SSIM. Using $1 - \rho$ as pooling weight, as in eq. (1), the correlation with MOS increases for all the three databases (see third and fourth columns of Table 1). For a better evaluation of the results, Table 1 also contains the correlation coefficients provided by three representative IQA metrics, namely the Visual Information Fidelity index (*VIF*) [13], the Visual Signal-to-Noise Ratio (*VSNR*) [20] and the Feature based similarity metric (*FSIM*) [19], on the three databases (6-8th columns of Table 1). *VIF* measures the mutual information between the original and degraded image using the a priori information on the distribution of wavelet coefficients of natural images. *VSNR* also employs the wavelet transform for computing contrast thresholds to measure the amount of contrast masking in order to assess and balance distortion visibility. *FSIM*, as mentioned at the beginning of Section 2, employs phase coherency and gradient magnitude in place of luminance adaptation and structural terms of SSIM; phase coherency is also used as pooling weight. As it can be observed in the Table, the proposed $\rho-$based correction to SSIM allows us to outperform *VSNR*, to approach and sometimes to outperfom *VIF*, while it is still not able to reach comparable results with FSIM in its present form, even though it is less computationally expensive and free of parameters. One of the most evident results in Table 1 is the great increment, especially in TID database, given by the use of ρ_{cos} as pooling weight for SSIM, as in eq. (2). Fig. 4 reports the scatter plot of the IQA metrics and MOS for TID database as well as the fitted logistic function. As it can be observed, crosses in the rightmost plot are better concentrated near the fitted curve. The Spearman correlation coefficient has been also measured separately for each degradation type and the results are provided in Table 2. As it can be observed, ρ_{cos} allows us to considerably increase the correlation of SSIM with MOS for degradations like non eccentricity patter noise, masked noise, quantization noise and jpeg compression. As mentioned in the previous

defect	$SSIM$	$SSIM_\rho$	$SSIM_{cos}$	FSIM
awgn	0.811	0.810	0.829	**0.857**
Diff noise in color	0.803	0.801	0.827	**0.851**
Spat. corr. noise	0.815	0.827	0.837	**0.848**
Masked noise	0.779	0.788	**0.811**	0.802
High freq. noise	0.873	0.875	0.888	**0.909**
Impulse noise	0.673	0.643	0.628	**0.746**
Quantization	0.853	0.857	**0.881**	0.855
Blur	0.954	0.957	**0.959**	0.947
Image den.	0.953	0.953	**0.962**	0.960
JPEG	0.925	0.917	**0.929**	0.928
JP2K	0.962	0.964	0.966	**0.977**
JPEG trans.	0.868	0.867	**0.887**	0.871
JP2K trans.	0.858	0.854	**0.866**	0.854
Non ecc. patt. noise	0.711	0.712	**0.763**	0.750
Local block. dist.	0.846	0.818	0.823	**0.850**
Mean shift	0.723	0.728	**0.734**	0.670
Contrast change	0.525	0.615	0.574	**0.65**

Table 2. Comparison of SCC provided by SSIM, $SSIM_\rho$, $SSIM_{cos}$ and FSIM [19] for each degradation kind in TID database (the best results are in bold).

section, pooling weights in eqs. (1) and (2) have been derived from the degraded image and not from the original image in order to be more sensitive to the unnatural elements introduced by the distortion. In fact, as shown in the rightmost part of Table 1, by estimating the pooling weights directly in the original image, the correlation of the proposed image quality metrics ($SSIM_\rho$ and $SSIM_{cos}$) with MOS still increases with respect to the conventional SSIM, but the increment is smaller than the one provided by the estimation of the pooling weights directly in the degraded image. Table 3 compares the correlation with MOS of $SSIM_{cos}$ and two representative existing and high performance IQA metrics, namely the percentile-fixations SSIM (PF-SSIM) [10] and the information content weighting SSIM (IW-SSIM) [17]. As it can be observed, the proposed IQA measure has similar performance of PF-SSIM, which reflects some mechanisms of vision but depends on parameters that are heuristically fixed. With regard to IW-SSIM, the proposed metric has comparable performance on LIVE database, while it is slightly inferior on TID database. It is worth mentioning that the success of IW-SSIM is due to the effective but expensive combination of several proven useful approaches in IQA research, such as multiscale image decomposition followed by scale-variant weighting, SSIM-based local quality measurement, and information theoretic analysis of visual information content and fidelity. On the contrary, the computation of the correlation coefficients in $SSIM_\rho$ or in $SSIM_{cos}$ requires a convolution with a linear filter on the squared luminance and contrast images, that, in turn, can be obtained using a simple convolution. This additional computational cost is only moderate. The latter point is not trivial for the actual use of pooled IQA metrics in real time processing, especially the ones involving a huge quantity of data.

	DB	$SSIM_{cos}$	PF-SSIM (MS)	IW-SSIM
PCC	TID	0.835	–	0.858
	LIVE	0.954	0.955	0.952
SCC	TID	0.838	–	0.856
	LIVE	0.958	0.947	0.957

Table 3. Comparison of $SSIM_{cos}$ with the multiscale version of PF-SSIM [10] and IW-SSIM [17] in terms of PCC and SCC on TID and LIVE databases.

4. FUTURE WORK

The current work represents an initial study concerning the use of the relation between luminance mean and contrast in weighting image information. In the future, more investigations are needed about the relationship between these two measures and on what is the best way to quantify it. A possibile way could be to investigate more on the relationship of the correlation coefficient with the mutual information and/or on the significance of the cosine correlation and its dependence on the ratio $\| * \|_1 / \| * \|_2$. Finally, the present study only uses SSIM as the base IQA metric due to its natural dependence on the two main measures that human eye computes during the observation process of an image. Future research will also apply the proposed pooling weights on other image quality assessment metrics.

5. REFERENCES

[1] B. P. Bondzulic and V. S. Petrovic, ”Additive models and separable pooling, a new look at structural similarity”, *Signal Processing*, 97, 2014.

[2] N.D.B. Bruce and J.K. Tsotsos, ”Saliency, attention, and visual search: An information theoretic approach”, *Journal of Vision*, 9(3),2009.

[3] V. Bruni, D. Vitulano, and G. Ramponi, ”Image quality assessment through a subset of the image data”, *Proc. of ISPA 2011*, IEEE 2011.

[4] D. Chandler and S. Hemami, ”VSNR: A Wavelet-Based Visual Signal-to-Noise Ratio for Natural Images”, *IEEE Trans. on Im. Proc.*, 16(9), 2007.

[5] R. Frazor and W. Geisler, ”Local luminance and contrast in natural images”, *Vision Research*, 46, 2006.

[6] E. Larson and D. Chaendler. Categorical image quality database. http://vision.okstate.edu/csiq.

[7] V. Monte, R. Frazor, V. Bonin, W. Geisler, and M. Corandin, ”Independence of luminance and contrast in natural scenes and in the early visual system”, *Nature Neuroscience*, 8(12), 2005.

[8] N. Ponomarenko and K. Egizarian. Tampere image database 2008. http://www.ponomarenko.info/tid2008.htm.

[9] H. R. Sheikh, K. Seshadrinathan, A. Moorthy, Z. Wang, A. Bovik, and L. Cormack, ”Image and video quality assessment research at live”, http://live.ece.utexas.edu/research/quality/.

[10] A.K. Moorthy and A.C. Bovik, ”Visual importance pooling for image quality assessment”, *IEEE Journal on Special Topics in Sig. Proc.*,3(2),2009

[11] S. Rezazadeh, S. Coulombe, ”A novel approach for computing and pooling Structural SIMilarity index in the discrete wavelet domain”, *Proc. of ICIP* 2009.

[12] A. Saadane, ”Towards a unified fidelity metric of still coded images”, *Journal of Elec. Imaging*, 2007.

[13] H. Sheikh, A. Bovik, ”Image information and visual quality”, *IEEE Trans. on Im. Proc.*, 15(2), 2006.

[14] R. Soundararajan and A. C. Bovik, ”Survey of information theory in visual quality assessment”, *Signal Image and Video Proc.*, 7(3), 2013.

[15] E.C.L. Vu, E.C. Larson, and D.M. Chandler. ”Visual Fixation Patterns when Judging Image Quality: Effects of Distortion Type, Amount, and Subject Experience”, *Proc. of SSIAI* 2008.

[16] Z. Wang, L. Lu, and A. Bovik, ”Video quality assessment based on structural distortion measurement”, *Signal Proc.: Image Comm.*, 19(2), 2004.

[17] Z. Wang and Q. Li, ”Information Content Weighting for Perceptual Image Quality Assessment”, *IEEE Trans. on Image Proc.*, 20, 2011.

[18] W. Xue, L. Zhang, X. Mou, and A. C. Bovik, ”Gradient Magnitude Similarity Deviation: An Highly Efficient Perceptual Image Quality Index”, to appear in *Computer Vision and Pattern Recognition*.

[19] L. Zhang, L. Zhang, X. Mou, and D. Zhang, ”FSIM: a feature similarity index for image quality assessment”, *IEEE Trans. Image Proc.*, 20(8), 2011.

[20] D. Chandler and S. Hemami, ”VSNR: A Wavelet-Based Visual Signal-to-Noise Ratio for Natural Images”, *IEEE Trans. on Im. Proc.*, 16(9), 2007.